Affine-invariant skeleton of 3D shapes

M. Mortara G. Patané
Istituto per la Matematica Applicata
Consiglio Nazionale delle Ricerche
{michela,patane}@ima.ge.cnr.it

Abstract

In the recent past, different application fields have showed an increasing interest in shape description oriented to recognition and similarity issues. Beyond the application aims, the capability of handling details separating them from building elements, the invariance to a set of geometric transformations, the uniqueness and stability to noise represent fundamental properties of each proposed model. This paper defines an affine-invariant skeletal representation; starting from global features of a 3D shape, located by curvature properties, a Reeb graph is defined using the topological distance as quotient function. If the mesh is uniform, this Reeb graph can be also viewed as a geometric skeleton defined by the barycenters of pseudo-geodesic circles sequentially expanded from all the feature points.

1 Introduction

Shape description is the basis for recognition and is one of the key problems for similarity (matching) and recognition issues. To this end, proposed methods should satisfy the fundamental criteria of invariance, uniqueness and stability to noise and computation. Another important property of a powerful shape descriptor is the capability of handling details, separating them from more essential shape characteristics; this can be achieved representing an object as a hierarchy of shape elements at different scales. This approach guarantees noise stability, which is achieved by ignoring the lower levels of the hierarchy, and allows top-down operations on the input object. It is not trivial to define a general shape descriptor which fulfils all these requirements at the same time, and ad hoc solutions have been proposed for specific applications. The Medial Axis Transformation (MAT) [4] is probably the best-known method for characterizing shapes, and it provides an integrated approach for the characterization and compression of shape information. The medial axis, together with the radius function, i.e. the distance from each point on the axis to the nearest one on the boundary, defines the MAT. The power of this representation is that the surface boundary and its MAT are equivalent and one can be computed from the other: therefore, a two-dimensional object is transformed into a one-dimensional graph-like structure. As described in [14], approximated versions of the MAT have been proposed to decompose a polygonal shape into a configuration of branches and protrusions. The medial axis is independent from the object position in space (i.e. it is affine- invariant), but it is not stable to small perturbations of the shape boundary. Furthermore, the medial axis of a 3D shape is more complex and contains not only lines but also surface elements. Another fundamental approach for the definition of a skeletal representation of surfaces is represented by the theory of Reeb graphs. Given a manifold, Reeb graphs can be constructed by studying the configuration of the critical points of a generic continuous function defined on the first one [16, 18] (see Figure 1(b)). In most applications the height function is chosen even if it has the main drawback of producing graphs which are dependent on the orientation of the object in space. To overcome these problems other maps, as the geodesic distance, can be chosen for the skeleton construction. These problems show that, as underlined in [20], a coordinate-independent shape description, able to distinguish between meaningful and detail features still lacks. Moreover, tools suggested to construct such a representation are related to geometric and topological information, e.g. curvature and geodesics, on the input surface. Starting from considerations mentioned above, we present an affine-invariant skeletal representation of triangular meshes which will be generalized to manifolds. The proposed (Reeb) graph is defined using the topological distance from global features, defined by curvature extrema, as chosen function on the input manifold.

2 Review of related work

The aim of skeleton extraction is to select and to convert shape characteristics and properties of the surface into a compact representation. One of the best known shape

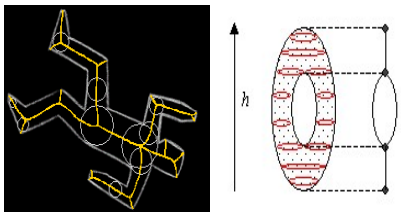

(a) (b)

Figure 1. (a) Medial Axis Transform, (b) Reeb graph with respect to the height function.

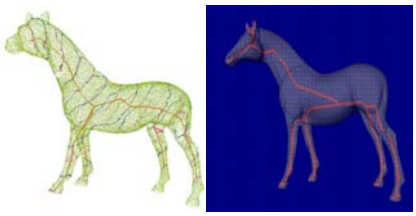

(a) (b)

Figure 2. (a) Level sets and skeletal curves computed on the horse point set, as shown in [12], (b) result obtained with our algorithm.

descriptors is the Medial Axis Transformation, defined by Blum in [4] for 2D shapes and extended to the 3D case by Sherbrooke [17]. In the planar case, the Medial axis of a shape is a graph defined as the locus of the centers of all the maximal discs contained inside the shape and having at least two points of contact with its boundary (see Figure 1(a)). It is known that this representation is independent of the object position in space (invariance), but has the negative side that tiny perturbations of the boundary produce extra edges in the graph, with no distinction between main and secondary features. Another method which is commonly used for shape description, and strictly related to our method, is the Reeb graph [1, 3, 16] whose definition is based on the Morse theory [13, 18]. First of all, Morse theory states that the topology of a given manifold M can be studied analyzing the critical points of any smooth function $h : M \to \mathbf{R}$. Typically, the map h represents the height function ($\forall p = (x, y, z) \in \mathbf{R}^3$, $h(x, y, z) = z$) whose critical points, i.e. peaks, pits and passes, are useful for shape description because they locate its basic elements. Starting from Morse theory, it is possible to define the Reeb graph [16] by coding the evolution of the "contours" on M defined by h as described by the following definition.

Definition. Let $h : M \mapsto \mathbf{R}$ be a real valued function on a compact manifold M. The *Reeb graph of M with respect to* h is the quotient space of $M \times \mathbf{R}$ defined by the equivalence relation $\sim$, given by $(p, h(p)) \sim (q, h(q))$, $p, q \in M$, if and only if

- $h(p) = h(q)$,
- p, q are in the same connected component of $h^{-1}(h(p))$.

Therefore, the Reeb graph can be represented as a 1-dimensional skeleton, provided by a continuous scalar function on M, which changes choosing different maps for the definition of $\sim$.

Even if different extensions of this theory [1, 3, 18] have been proposed, the Reeb graph suffers of at least two problems. Firstly, it depends on the chosen map h and, secondly, there is no distinction between large and small features due to the fact that the same connected components are collapsed into the same class without distinction of their sizes. Because the height function h is not affine-invariant, in [10] a new map, based on the geodesic distance from a source point $p \in M$, has been defined to overcome this problem. The determination of p is not simple; the solution proposed by the authors is to define, for every $x \in M$, $h(x)$ as the sum of all geodesic distances $g(x, p)$ from x to p when p varies on the input manifold. A similar approach to that described here deals with the construction of centerlines from unorganized point sets [12], later developed for polyhedral objects [11]. With particular reference to [11], a 1-dimensional axial structure for genus 0 triangular meshes is presented, which is essentially a tree made of the "average points" associated with the connected components of the level sets of a given function; in particular, the shortest distance to a source point is chosen. To automatically select the source point an heuristic is used which seems to work well on elongated shapes (like the horse ears in Figure 2. Anyway the choice of only one source point determines a privileged "slicing direction", which can lead to the loss of some features if the object is not tubular shaped (see Figure 2). We use here a similar approach, which selects at first all the meaningful features as "source points" to start the skeleton construction, fact that prevents from loss of desired information.

3 Overview of the technique and contributions

The proposed construction of the skeleton of a 3D object represented by a triangular mesh is made in 3 steps.

1. A gaussian curvature estimation is performed on the mesh and several zones of high curvature, which identify the surface features, are extracted (see Figure 3(a)). Since curvature is an intrinsic characteristic of

the surface, a curvature-based skeleton is coordinate independent. The curvature estimations is performed using a novel technique, which is described in [7]. The idea is to detect points which identify ”global” curvature features and to create a hierarchy of such elements related to their scale.

2. Starting simultaneously from the centroid of the high curvature regions, topological rings consisting of vertices which have the same topological distance (minimum number of edges) from the nearest centroid are computed, growing of one edge at a time, until the whole surface is covered (see Figure 3(b)).

3. The graph is constructed. The centroids of high curvature regions become the terminal nodes of the graph, while points of split or collision between topological rings during the expansion phase individuate the branching nodes. The centroids of the topological rings between two nodes are connected to form an edge (see Figure 3(c)).

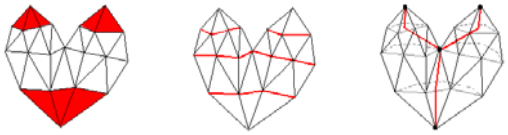

(a) (b) (c)

Figure 3. Main steps of the algorithm: (a) curvature evaluation, (b) topological expansion, (c) graph construction.

The definition of gaussian curvature for meshes is not trivial because they are parameterized by piecewise continuous functions whose second derivatives are, almost everywhere, null. Among the different approaches which have been used to overcome the lack of a standard definition two main algorithms can be identified. The first one [9] ([19]) derives its discrete approximation at each vertex applying its continuous definition (i.e. estimating the tensor curvature) to a least-square paraboloid fitting its neighboring vertices. The second one [5] is based on the Laplace-Beltrami operator and the Gauss map guaranteing the validity of differential properties such as area minimization and mean curvature flow [8].

In spite of the introduction of a multi-resolution structure, all the previous approaches are usually sensitive to noise and small undulations requiring smoothness conditions on the input mesh. Furthermore, the smoothing process used to get stable and uniform curvature estimations introduces a deficiency in the magnitude evaluation and, consequently, difficulties in the accurate distinction between

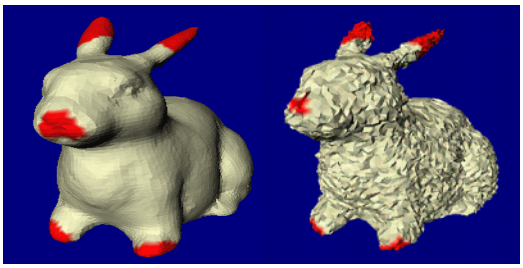

(a) (b)

Figure 4. Approximated gaussian curvature estimation on the rabbit: red regions indicate high-curvature areas. In (b) a gaussian noise has been added to input points.

planar patches and curved surfaces with low curvature. Conversely, we need a classification of points which takes into account both curvature extrema and the related shape size in order to identify global features of maximal curvature which represent the input of our algorithm for shape abstraction. Curvature evaluation can also be defined by an angle associated with a closed path on the surface, i.e. the *angle excess* [15], defined as the total turning that a reference pointer undergoes when carried around a closed path. Angle excess is additive and the following theorem applies: for any topological disk on an arbitrary surface, the angle excess around the boundary is equal to the total curvature of the interior. It follows that a region on an arbitrary surface can be divided into pieces, and the sum of the excess angles of all these subparts of the subdivision gives the total curvature of the region, which precisely equals to the excess around the region boundary. These considerations represent the starting point of the framework used for curvature evaluation on triangular meshes [7]. In Figure 4 (a), an example is shown where red areas identify high-curvature features; an example of the algorithm robustness to noise is given in Figure 4(b). The paper is organized as follows: steps 2 and 3 are described in detail in section 4. The mathematical definition of the graph as a quotient space is given in section 5, while its properties and a comparison with the Reeb graph are provided in section 6. Future work and results are presented in the last section.

4 Graph construction

Any object can be seen as essentially made of a main body with several protrusions: for instance, the overall shape of a man consists of the torso from which head, arms and legs depart. From this point of view, the main features of a 3D surface are its protrusions, and these ones are detectable by mean of gaussian curvature: at a protrusion ex-

tremity there must be a high curvature region. Following these considerations, we are going to construct the skeleton of a 3D surface as a curvature-based graph which, starting from high curvature regions, grows inside the shape towards the main body according to the mutual adjacency between features. High curvature regions are extracted as described in [7]; we will show in this section how the developed algorithm constructs the graph edges and determines the branching nodes according to a topological expansion method. We represent a triangular mesh S as the pair $S := \{V, F\}$ where $V := \{p_i = (x_i, y_i, z_i) : i = 1, \ldots, N\}$ is a list of N vertices and F is an *abstract simplicial complex* [6] which contains the adjacency information whose subsets come in three types: vertices $\{i\}$, edges $\{i, j\}$ and faces $\{i, j, k\}$. The topology in S is defined by F in the sense that we can construct the *1-neighborhood* structure as

$$\{N(i) : i = 1, \ldots, N\} \tag{1}$$

with

$$N(i) := \{j \in \{1, \ldots, N\} : (i, j) \in F\}.$$

The previous relation assigns to each vertex i the set of its 1-neighborhood, that is, the vertices j such that (i, j) is an edge of the triangulation F. The size (radius) of the neighborhood structure can be recursively enlarged by defining a *n-neighborhood* (see Figure 5) as

$$\begin{array}{l} N(i_i, \ldots, i_k) := \bigcup_{l=1}^{k} N(i_l), \\ N^0(i) := \{i\}, \\ N^1(i) := N(i), \\ N^n(i) := N^1(N^{n-1}(i)),\ n \geq 2. \end{array} \tag{2}$$

Therefore, given a vertex $i \in \{1, \ldots, N\}$ we can define its *local neighborhood system* as

$$B_i := \{T(N^k(i)) : k = 0, \ldots\}$$

with

$$T(N^k(i)) := \bigcup_{l,p,q \in N^k(i), \{l,p,q\} \in F} T(l, p, q)$$

and $T(l, p, q)$ the triangle with vertices l, p, q. Finally, we refer to the border of $T(N^k(i))$, i.e. $\partial T(N^k(i))$, as *topological ring of order k for i*.

From the previous definitions the following conditions hold: $\forall i \in \{1, \ldots, N\}$

- $v_i \in T(N^k(i)), \qquad k = 0, \ldots$
- $T(N^k(i)) \subseteq T(N^{k+1}(i)), \qquad k = 0, \ldots$
- if S is connected, then

$$S = \bigcup_{k=1,\ldots} T(N^k(i)).$$

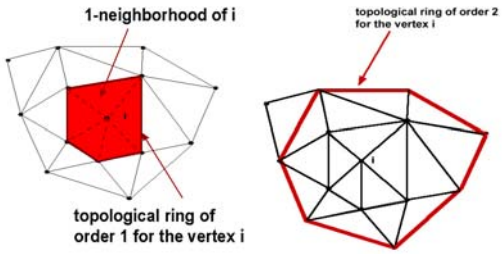

(a) (b)

Figure 5. Local neighborhood system on a triangular mesh: topological ring of order 1 (a), and (b) of order 2 for i.

4.1 Topological expansion

Once computed the approximated gaussian curvature for the mesh vertices, for each high curvature region R_i a representative vertex p_i is selected (for a more pleasant visualization p_i is chosen as the centroid of R_i and computed as the farthest vertex from the region boundary; anyway, we underline that from the topological point of view the choice of p_i is irrelevant). Each point in the set $\{p_i\}$ represents the terminal nodes of the graph. Starting from $\{p_i\}$, we can construct a skeleton of the object following a topological expansion approach, based on the idea of topological rings growing (expanding) from representative vertices and traversing the mesh, until rings split, collide with others, or can be expanded no more. Starting at the same time from all the representative vertices, the topological rings expand one step at a time until:

- rings belonging to different representative vertices collide: a union occurs,
- a ring intersects itself: a split occurs,
- a ring can be expanded no more: the ring terminates.

Union. When expanding a topological ring we meet a vertex already belonging to the topological ring (of the same order) of another representative vertex, the two rings intersect. From the point of view of the surface, this means that we have found a branching zone of the object where two distinct protrusions depart (see Figure 6). In the same way, the corresponding skeleton will have a branch with two edges joining. The rings of the representative vertices, which determined the collision, can be expanded no more and the construction of their ring sets is completed. A new topological ring is created for the intersection vertex; in this case, unlike what happens for representative vertices, the firstly coded topological ring is the union of the two rings colliding.

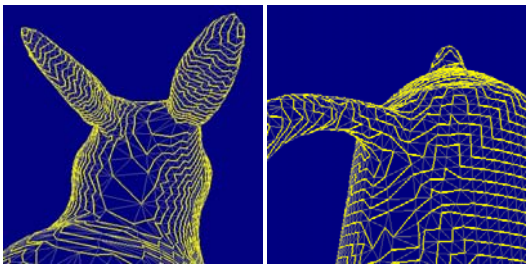

(a) (b)

Figure 6. (a) Example of union, and split (b).

Split. It can also happen that a ring intersects itself in one or more of its vertices; this is the situation of rings expanding near handles, through holes of the object or where a new protrusion starts. In this case, the intersecting ring splits in two parts and its expansion stops in favor of two new rings derived from the split (see Figure 6(b)).

Termination. After a finite number of steps, the splitting and joining rings will cover the whole surface. A ring terminates when the next step would produce a non valid boundary, that is, with less than 3 vertices. When a ring terminates, it means that there were no more significant features in the object. Therefore, branches of the skeleton will be not produced in the case of a ring which terminates without having a union or a split.

When all the ring sets of the representative vertices and the ones created during their expansion are terminated, the algorithm can draw the skeleton as the adjacency graph encoded during the expansion phase (see Figure 7):

- each representative vertex gives a *terminal node*,
- each union or split of topological rings gives a *branching node*,
- the topological rings, belonging to the ring set of a node, give an arc which goes out from that node [1]. In particular, an arc is drawn joining the center of mass of all its topological rings.

5 Graph as quotient space

In this section we are concerned with the formulation of the graph construction for triangular meshes and manifolds demonstrating that it is the quotient space of the input object surface S with respect to an equivalence relation $\sim$. The proposed construction of G as $S/\sim$ enables to:

[1]Note that when a split or a union occurs, there can be two arcs going off the same node: in this case, two distinct ring sets are created for the same node. Therefore, each ring set always defines one node and one arc.

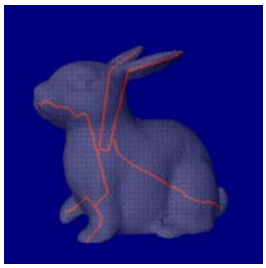

Figure 7. Example of skeleton on the rabbit.

- verify that G only depends on the topology of S and on a finite set of representative points $\{p_1,\ldots,p_n\}$ in S of high-curvature values,
- verify that G is affine-invariant; this characteristic represents one of the main properties of G and of this theory not shared by other approaches,
- extract the information on G (e.g. compactness, connectivity, etc.) starting from S and exploiting the properties of the quotient space.

5.1 Graph definition for triangular meshes

Selected a point p_i in S, we introduce the function

$$f_{p_i} : S \to \mathbf{N}$$
$$x \mapsto f_{p_i}(x) := \min\{k : x \in T(N^k(i))\}$$

, i.e., $f_{p_i}(x)$ is the minimal *topological distance* between p_i and x. We can extend in a simple way the previous function to a finite set of vertices $\{p_1,\ldots,p_n\}$ as

$$f : S \to \mathbf{N}$$
$$x \mapsto f(x) := \min_{k=1,\ldots,n}\{f_{p_k}(x)\}$$

, i.e., f assigns to x its minimal topological distance with respect to more than one vertex ($n = 1, f = f_{p_1}$).

Starting from f and S we are able to construct the relation $\sim$ as follows (see Figure 8):

$$p,q \in S,\ p \sim q \text{ iff } f^{-1}(f(p)) \cap f^{-1}(f(q)) \neq \emptyset. \quad (3)$$

First of all, (3) implies that if $f(p) \neq f(q)$ then $p \not\sim q$; in fact, we have

$$f^{-1}(f(p)) \cap f^{-1}(f(q)) = f^{-1}(\{f(p)\} \cap \{f(q)\}) = \emptyset.$$

In other words, necessary condition for $p \sim q$ is that $f(p) = f(q)$, that is, p and q have the same topological distance from the selected set of vertices $\{p_1,\ldots,p_n\}$. Furthermore, two points p and q are in relation with respect to $\sim$ if and only if they have non-disjoint topological rings (i.e. $f^{-1}(f(p)) \cap f^{-1}(f(q)) \neq \emptyset$) of the same order (i.e. $f(p) = f(q)$).

Now we want to investigate the properties of $\sim$:

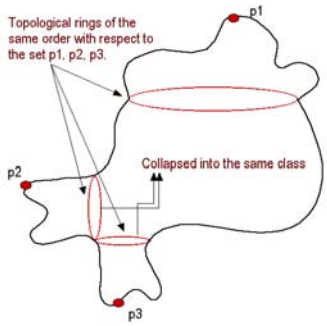

Figure 8. Topological rings on a manifold.

- reflexive: $\forall p \in S, p \sim p$,
- symmetric: $\forall p, q \in S, p \sim q \Rightarrow q \sim p$,
- transitive: $\forall p, q, r \in S, p \sim q, q \sim r \not\Rightarrow p \sim r$. In fact, the intersection of sets is not transitive on $P(X) := \{X : X \subseteq S\}$.

From the previous relations it follows that

$$G = S/\sim = \{[x] : x \in S\}$$

where the class of x is represented by the set

$$[x] := \{y \in S : y \sim x\}.$$

Furthermore, the following conditions hold:

- $[x] \neq \emptyset, \forall x \in S$ (i.e. every class is not empty),
- $x \sim y \Rightarrow [x] \cap [y] \neq \emptyset$ (i.e. two vertices which satisfy the relation $\sim$ have non-empty intersection. Generally, the inverse condition is not true because $\sim$ is not transitive.),
- $\bigcup_{x \in S}[x] = S$ (i.e. $\{[x]\}_{x \in S}$ represents a cover of S).

5.2 Graph definition for manifolds

We want to extend the previous model to a compact manifold without boundary embedded in $\mathbf{R}^3$ with the Euclidean topology underlining the general application of our model for the extraction of an affine-invariant shape description. In the following we review definitions and concepts on topology introducing the basic notions and referring to [6] for further readings. The structure of the section reflects that of the previous one facilitating the parallelism between the continuous case study and the discrete one which has been used for the implementation of the algorithm.

Introduced a topological space (X, τ), we define as

- *induced topology of X in $S \subseteq X$*: the topology τ_S defined as

$$\tau_S := \{A \cap S : A \in \tau\},$$

- *local base of p in X*: the family B_p consisting of neighborhoods of the point p such that for every neighborhood U of p there is a set $V \in B_p$ such that $V \subseteq U$,
- *boundary of $A \subseteq X$*: $\partial A := \overline{A} \cap \overline{X - A}$, that is, the intersection between the closure of the set A and of its complement $(X - A)$ in X.

Given a point $p \in S$ we define, for every $R > 0$, the open ball of center p and radius R as

$$B(p, R) := \{x \in \mathbf{R}^3 : ||x - p||_2 < R\}$$

and with $U(p, R)$ the connected component of p in $S \cap B(p, R)$. Therefore, we can associate to each point $p \in S$ the family of neighborhoods $\{U(p, R)\}_{R>0}$. From the previous relations we can derive the following properties which will be used for constructing the graph of S:

- $\{U(p, R)\}_{R>0}$ is a local base of the space S at the point p with respect to the topology τ_S induced by the Euclidean topology τ in S. This property follows using the definition of τ_S and the fact that the set $\{B(p, R)\}_{R>0}$ is a local base of p in $(\mathbf{R}^3, \tau)$.
- $R_1 < R_2 \Rightarrow U(p, R_1) \subseteq U(p, R_2)$: in fact, $R_1 < R_2 \Rightarrow B(p, R_1) \subseteq B(p, R_2) \Rightarrow S \cap B(p, R_1) \subseteq S \cap B(p, R_2) \Rightarrow$ the connected component of p in $S \cap B(p, R_1)$ is a subset of that in $S \cap B(p, R_2)$.

Introduced the counterparts of the concepts defined for the triangular mesh, we can extend the previous functions as described in the following. Chosen a point $p \in S$, we define the map

$$\begin{aligned} f_p &: \mathbf{R}^3 \to \mathbf{R} \\ & x \mapsto f_p(x) := ||p - x||_2 \end{aligned}$$

and then, fixed a set of points $P := \{p_1, \ldots, p_n\} \subseteq S$, we construct its extension to the set P as

$$\begin{aligned} f &: S \to \mathbf{R} \\ & x \mapsto f(x) := \min_{k=1,\ldots,n}\{f_{p_k}(x)\}. \end{aligned}$$

The function f is continuous because it is the composition of the continuous maps

$$\begin{aligned} (f_{p_1}, \ldots, f_{p_n}) &: S \to \mathbf{R}^n \\ & x \mapsto (f_{p_1}(x), \ldots, f_{p_n}(x)) \end{aligned}$$

and

$$\begin{aligned} \min &: \mathbf{R}^n \to \mathbf{R} \\ & (x_1, \ldots, x_n) \mapsto \min_{i=1,\ldots,n}\{x_i\}. \end{aligned}$$

Therefore, in analogy with the previous section, we can introduce the relation $\sim$ as: $p, q \in S$, $p \sim q$ if and only if we can choose $R > 0$ such that $f(p) = f(q)$ and p, q belong to the same connected component of $f^{-1}(f(p))$. In other words, necessary and sufficient condition for $p \sim q$ is that p and q have the same topological distance from the selected set of points $\{p_1, \ldots, p_n\}$ and they belong to the connected component of the pre-image of their (common) value $f(p)$. The relation $\sim$ is symmetric, reflexive and transitive because it is the intersection of two equivalence relations (i.e. function equality and membership to the same connected component). Using the properties of the quotient space, we deduce that $\sim$ induces in S a decomposition into a family of non-empty, disjoint topological classes. If the input surface S is compact/connected then G is compact/connected; anyway, the canonical projection

$$\begin{aligned} \pi : S &\mapsto G = S/\sim \\ x &\mapsto [x] \end{aligned}$$

is continuous with respect to the quotient space topology (i.e. $A \subseteq G$ is open if $\pi^{-1}(A)$ is open in (S, τ_S)).

6 Properties and comparison

In this section we want to present the main properties and distinctions of the graph G with respect to the Reeb graph constructed by using the height function. This comparison is evaluated considering the topological properties of both graphs, as quotient spaces, and a set of experimental results which underline the main drawbacks of the previous theory for shape abstraction.

The complexity of the proposed graph, in terms of number of nodes and branches, depends on the shape of the input object and on the number of points $\{p_i\}_{i=1}^{n}$ which we have selected using the curvature estimation criterion. The construction of G is guided, in the first step, by the topology of the mesh through the connectivity relations in F and, secondly, by the geometry V which influences the chosen representative point p for its equivalence class $[p]$. If the mesh is uniform, i.e. all the edges have nearly the same length, the topological rings are more balanced and the resulting skeleton is smoother; otherwise, it is possible to pre-process the mesh applying a regularization and/or a refinement algorithm [2] to get better results (see Figure 9). Our graph is affine-invariant (translation, rotation, scaling and shear) because the chosen function f does not rely either on a local coordinate system or on surface embeddings as it happens, for example, using the height function. On the other hand, if the curvature evaluation process does not recognize at least one feature region (e.g. surfaces with constant curvature values such as spheres and torii), our approach is not useful to extract a description of the shape; on the contrary, the height function always guarantees to get a result. The

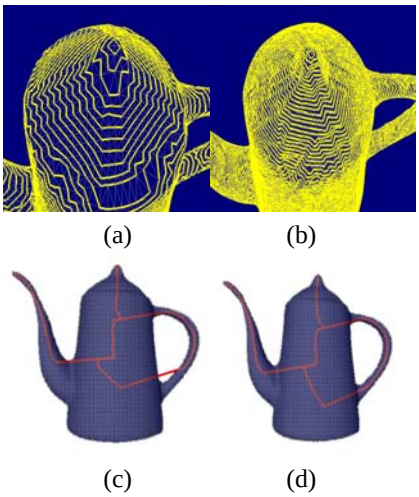

Figure 9. (a) Topological rings on the input, (b) on the refined mesh, (c) skeleton of (a), (d) skeleton of (b).

graph construction is also allowed for 3D-shapes of genus greater than zero (see Figure 9). An interesting question is: does a relation between them exist? In other words, which hypothesis on S ensures that the related quotient spaces are homeomorphic?

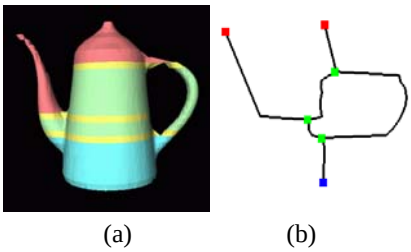

Figure 10. (a) Characterization of the pot in maximum, minimum and saddle areas [1], (b) Reeb graph with respect to the height function.

7 Conclusions and future works

The starting point of this work is represented by previous approaches on shape abstraction attempting to propose possible extensions of the Reeb graph which is the core of our model. The presented graph is the first step toward the construction of a complete framework for shape abstraction, analysis and comparison. One of the most involving applications that we foresee and we want to approach is shape

matching. The affine-invariant structure of this graph and its description as quotient space enable to convert the matching problem between two graphs G and H into a multiple framework whose solution is achieved by defining a matching function which is a homeomorphism between G and H plus a penalty function which takes into account the geometry of the objects associated to them.

8 Acknowledgements

Special thanks are given to B. Falcidieno and the Computer Graphics Group at IMA-CNR for the support and contributions to the development of described results. We would also like to thank who significantly contributed to the ideas presented in this paper: J. Rossignac, with whom we started an interesting research on curvature analysis, and G. Wyvill who suggested the use of geodesic expansion.

References

[1] M. Attene, S. Biasotti and M. Spagnuolo, "Remeshing Techniques for Topological Analysis", *Proceeding of Shape Modeling International 2001*, IEEE Press, Genoa, May 2001, pp.142-151.

[2] M. Attene, G. Wyvill, "Mapping independent triangulation of parametric surfaces", *Tech Sketch, SIGGRAPH 2001 Conference Abstracts and Application*, pp. 224.

[3] S. Biasotti, B. Falcidieno and M. Spagnuolo, "Extended Reeb Graphs for Surface Understanding and Description", in *Proceedings of the* 9^{th} *Discrete Geometry for Computer Imagery Conference, LCNS*, Springer Verlag, Uppsala, 2000.

[4] H. A. Blum, "Transformation for Extracting New Descriptors of Shape", *Models for Perception of Speech and Visual Form*, MIT Press 1967, 362-381.

[5] M. Desbrun, M. Meyer, P. Schroeder, A.H. Barr, "Discrete Differential-Geometry Operators in nD", July 22, 2000. URL: http://www.multires.caltech.edu/pubs/pubs.htm

[6] R. Engelking and K. Sielucki, *Topology: a geometric approach*, Sigma Series in Pure Mathematics, Volume 4, Heldermann Verlag, Berlin, 1992.

[7] B. Falcidieno, M. Mortara, G. Patané, J. Rossignac, M. Spagnuolo, *Tailor: understanding 3D shapes using curvature*, Technical Report 9/2001, Istituto per la Matematica Applicata, Consiglio Nazionale delle Ricerche.

[8] V. Guillemin, and A. Pollack, *Differential Topology*, Englewood Cliffs, NJ: Prentice-Hall, 1974.

[9] B. Hamman, "Curvature Approximation for Triangulated Surfaces", *Computing Suppl.* 8, 1993, pp. 139-153.

[10] M. Hilaga, Y. Shinagawa, T. Kohmura, T.L. Kunii, "Topology Matching for Fully Automatic Similarity Estimation of 3D Shapes", *Computer&Graphics, Proceeding of Siggraph 2001*, Los Angeles, 2001.

[11] F. Lazarus, A. Verroust, "Level Set Diagrams of Polyhedral Objects", *ACM Solid Modeling '99*, Ann Arbor, Michigan, USA.

[12] F. Lazarus, A. Verroust, "Extracting skeletal curves from 3D scattered data", *The Visual Computer*, vol. 16, N. 1, pp 15-25, 2000.

[13] J. Milnor, *Morse Theory*, Princeton University Press, New Jersey, 1963.

[14] M. Mortara and M. Spagnuolo, *Hierarchical Representation of 2D Polygons based on Approximate Skeletons*, Technical Report N. 8/2000, Istituto per la Matematica Applicata, Consiglio Nazionale delle Ricerche.

[15] M. E. Mortenson, *Geometric Modeling*, John Wiley & Sons, 1985.

[16] G. Reeb, "Sur les points singuliers d'une forme de Pfaff completement integrable ou d'une fonction numerique", *Comptes Rendus Acad. Sciences*, Paris, 1946, 222:847-849.

[17] E. C. Sherbrooke, N. M. Patrikalakis and E. Brisson, "An Algorithm for the Medial Axis Transform of 3D Polyhedral Solids", *IEEE Transaction on Visualization and Computer Graphics*, Vol. 2, N.1, March 1996.

[18] Y. Shinagawa, T.L. Kunii, and Y.L. Kergosien, "Surface Coding Based on Morse Theory", *IEEE Computer Graphics & Applications*, 1991, pp. 66-78.

[19] G. Taubin, "Estimating the Tensor Curvature of a Surface from a Polyhedral Approximation", *Fifth International Conference on Computer Vision (ICCV'95).*

[20] G. Wyvill and C. Handley, "The 'Thermodynamics' of Shape", *Proceedings of Shape Modeling International 2001*, IEEE Press, Genoa, Italy, May 2001, 2-8.

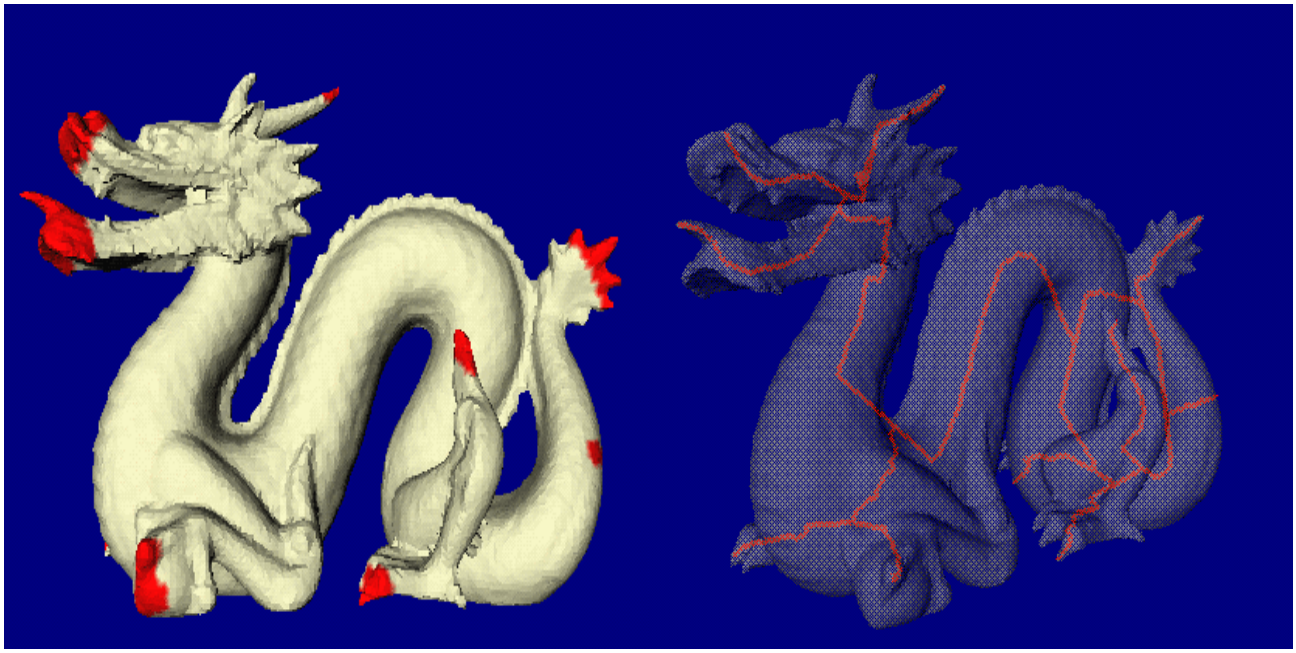

Color plate1: curvature estimation on the dragon, and skeleton construction

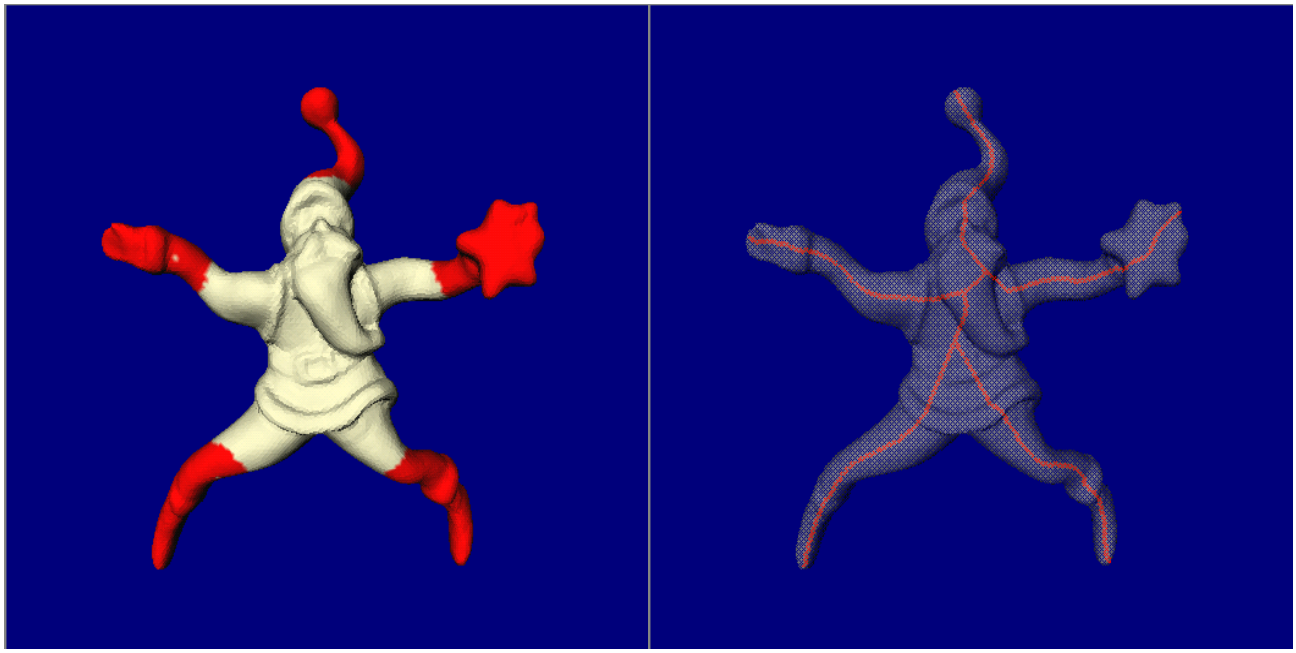

Color plate2:Curvature estimation on Santa Klaus and skeleton construction